How Can an Appropriate CFD Model be Developed for Turbulent Flow in Rough Pipes?: Evidence from Friction Factor Prediction

Kraiwit Boonsamer, Barami Temsiriphan, Piyawut Thongnoi, Surat Areerat, Eakarach Bumrungthaichaichan* and Santi Wattananusorn

Department of Chemical Engineering, School of Engineering, King Mongkut's Institute of Technology Ladkrabang, Bangkok, 10520, Thailand

How Can an Appropriate CFD Model be Developed for Turbulent Flow in Rough Pipes?: Evidence from Friction Factor Prediction

Kraiwit Boonsamer, Barami Temsiriphan, Piyawut Thongnoi, Surat Areerat,
Eakarach Bumrungthaichaichan[*] and Santi Wattananusorn

Department of Chemical Engineering, School of Engineering, King Mongkut's Institute of Technology Ladkrabang, Bangkok, 10520, Thailand

ABSTRACT

This paper answers the question: "How can an appropriate turbulent rough pipe flow computational fluid dynamics (CFD) model be developed?" The Reynolds-averaged Navier-Stokes equations with the standard k-epsilon turbulence model and scalable wall functions were solved to obtain Fanning friction factors and mean velocity profiles in inflectional and monotonic rough pipes. CFD models with near-wall grid sizes from four dimensionless wall distances and two roughness treatment approaches were simulated. Eight roughness Reynolds numbers, covering the lower end of the transitionally rough regime through the fully rough regime, were studied for each roughness type. Appropriate roughness and turbulence model constants for turbulent rough pipe flows in the transitionally rough regime were determined. For model validation, the predicted mean axial velocity profiles for Reynolds numbers of 5×10^4 and 5×10^5 exhibited good agreement with the reference experimental data. A total of 208 CFD simulations (32 from our previous works and 176 from the present study) were analyzed. Finally, based on comparisons between predicted Fanning friction factors and established correlations, appropriate CFD models for turbulent flows in inflectional and monotonic rough pipes were identified. Suitable CFD models for accurately predicting mean velocity profiles at roughness Reynolds numbers below 11.225 were also obtained, although with the caution that improved mean velocity prediction may reduce Fanning friction factor accuracy. Furthermore, the present CFD work provides essential guidance for extending simulations to other rough surface types and rough-wall flow situations.

1 Introduction

Roughness is one of the important effects on wall-bounded flows, e.g., flow in a pipe. This effect has been studied by many researchers, especially for turbulent flow. Over 90 years ago, Nikuradse [1], a hydraulic experimenter [2], studied the sand grain roughness effect on circular pipe flow. His invaluable experimental data have been considered and employed by many researchers up to the

---

1

K. Boonsamer, B. Temsiriphan, P. Thongnoi, S. Areerat, E. Bumrungthaichaichan
and S. Wattananusorn,
How can an appropriate CFD model be developed for turbulent flow
in rough pipes?: Evidence from friction factor prediction,
Rev. int. métodos numér. cálc. diseño ing. (2026). Vol.42, (2), 69

present. For example, Gioia and Chakraborty [3] used Kolmogórov's phenomenological theory to model the friction factors reported by Nikuradse [1]. In 1939, Colebrook [4] contributed to this research field through his work on the effect of commercial pipe roughness. Later, Moody [5] presented the friction factor in a convenient form of a graph for engineering applications by plotting the Darcy friction factor (f_D), noting that $f_D = 4f_F$, where f_F is the Fanning friction factor. Moody's friction factor curves for rough surface pipes revealed that friction factors decreased with increasing Reynolds number (Re) and asymptotically approached a constant value at higher Reynolds numbers. It is noted that, for pipe flows, $\text{Re} = DU/\nu = \rho DU/\mu$, where D is the pipe diameter, U is the average velocity, ν is the fluid kinematic viscosity, ρ is the fluid density, and μ is the fluid viscosity. This characteristic of the friction factor curve is called "monotonic roughness curve".

Although the Moody's diagram successfully represented a monotonic roughness curve, McGovern [6] later prepared the friction factor diagram by including monotonic and inflectional roughness curves. For the inflectional roughness curve, as the Reynolds number increases, the friction factor decreases to the minimum friction factor value and later increases again in the transitionally rough regime, finally approaching the constant value in the completely rough regime. Both artificial sand grain rough surface [1] and honed surface [7] produced inflectional characteristics. The McGovern's diagram [6] was constructed by incorporating von Kármán, Prandtl, Nikuradse expression for smooth pipe, Colebrook-White equation [4] for monotonic roughness curves, Afzal correlation [8] for inflectional roughness curves, and von Kármán expression for rough surface pipe at infinite Reynolds number.

The study of roughness effect on fluid flow is not limited to experimental and theoretical fluid dynamics techniques but has also been extended to computational fluid dynamics (CFD) due to significant improvement in computing performance and CFD's advantages [9]. These reasons encourage many researchers to investigate roughness effects in simple channel flows and more complex flow scenarios, such as gas cyclone separator [10,11], heat exchanger [12,13], etc., by CFD technique.

For pipe flow, Ibrahim et al. [14] used CFD-ACE, a finite volume method (FVM) based-CFD code, to investigate the roughness effect of a series of square-shaped, small tooth-like structures on laminar pipe flow by two-dimensional axisymmetric CFD simulation. Their results revealed that the pressure drop was found to increase, whereas the Nusselt number (Nu), representing heat transfer, was found to decrease, with increasing surface roughness. In 2010, Vijiapurapu and Cui [15] compared the capability of Reynolds-averaged Navier-Stokes (RANS) equation-based turbulence models, including k-epsilon model, k-omega model, and Reynolds stress model (RSM), and large eddy simulation (LES) for simulating three-dimensional fully developed flows in a circular pipe roughened by repeated square ribs. For time-averaged flow property prediction, the performance of all considered turbulence models was insignificantly different. LES was superior in predicting flow separation but required a higher computational cost.

Johansson [16] studied the sand grain roughness effect on pressure drops in Delrin, steel, and iron straight pipes as well as free form fabrication pipe with two and three bends by using experiments and CFD simulations with AVL FIRE, a commercial FVM-based CFD software. The near-wall grid (NWG) size was controlled by using dimensionless wall distance (y^+), which is generally defined as $yu_\tau/\nu = \rho yu_\tau/\mu$, where y is the normal distance from the wall and u_τ is the friction velocity and is defined as $\sqrt{\tau_w/\rho}$, τ_w is the wall shear stress. The study concluded that accurate pressure drop predictions were obtained by the near-wall grid size of at least twice the roughness height (k_s). Moreover, at least two cell layers were required to resolve the internal turbulent boundary layers. For identical simulation setups, either AVL FIRE or ANSYS Fluent can be used to predict similar

K. Boonsamer, B. Temsiriphan, P. Thongnoi, S. Areerat, E. Bumrungthaichaichan
and S. Wattananusorn,
How can an appropriate CFD model be developed for turbulent flow
in rough pipes?: Evidence from friction factor prediction,
Rev. int. métodos numér. cálc. diseño ing. (2026). Vol.42, (2), 69

compressible and incompressible internal flow results. Haroon et al. [17] simulated turbulent flows with Reynolds numbers from 5×10^3 to 10^7 in rough PVC, steel, and cast-iron pipes by using ANSYS CFX, a commercial FVM-based CFD code, with the standard k-epsilon turbulence model (hereafter standard k-epsilon model) and convergence criterion based on residuals of 10^{-5}. The simulated results showed that the standard k-epsilon model was adequate for predicting friction factors and head losses in rough pipe flows.

Abdelrazek et al. [18] investigated the effects of nanofluids' thermophysical properties on heat transfer and pressure drop through experiments and two-dimensional axisymmetric CFD simulations by using ANSYS Fluent, a commercial FVM-based CFD software, with the standard k-epsilon model. Reynolds numbers ranging from 6000 to 12,000 were studied. Their predicted average Nusselt numbers and pressure drops for distilled water agreed well with their experimental data, having an average error of about 5%. Later, Aldlemy et al. [19] used the experimental data of Abdelrazek et al. [18] for validating their CFD model and numerically investigated the pressure drops of turbulent rough pipe flows with the Reynolds number range from 5000 to 15,000 by using ANSYS Fluent with the standard k-epsilon model. The pipe flow CFD models of Aldlemy et al. [19] provided a higher average error than those of Abdelrazek et al. [18]. They concluded that the roughened pipes provided more effect on pressure drop than the smooth pipe.

Loyseau et al. [20] numerically investigated flow and turbulence fields inside 0.5 inch, 14.5 inch, and 48 inch-diameter pipes by using BL-v^2/k turbulence model of Code_Saturne, k-epsilon model of Code_Saturne, k-omega SST of Code_Saturne, OpenFOAM, and ANSYS Fluent, and RSM of ANSYS Fluent. They used the Fanning friction factor for smooth turbulent pipe flow of the Blasius correlation [21], cooperated with different dimensionless wall distance values, which depended on the turbulence model, to estimate near-wall grid sizes. It is noted that, from definitions of dimensionless wall distance and Fanning friction factor ($f_F \equiv 2\tau_w / (\rho U^2)$), the normal distance between the wall and computing node of the first near-wall grid (y_p) can be calculated by Eq. (1), which is commonly used for estimating the near-wall grid size of turbulent pipe flow CFD simulation.

$$y_p = \frac{y^+ \nu}{U\sqrt{f_F/2}} = \frac{y^+ \mu}{\rho U \sqrt{f_F/2}} \tag{1}$$

The near-wall grid sizes for vertex-based CFD codes (e.g., ANSYS CFX) and cell-center-based CFD codes (e.g., ANSYS Fluent, AVL FIRE, etc.) are y_p [9] and $2y_p$ [9,22], respectively. The simulated results for the 14.5 inch-diameter pipe confirmed that RSM was better than other turbulence models because it accounts for anisotropic turbulence but required higher computing costs. Moreover, the k-omega SST model was recommended for three different pipe sizes due to its reasonably good prediction accuracy.

Temsiriphan [23] proposed a concept for determining the appropriate dimensionless wall distance, i.e., y^+, required to estimate near-wall grid sizes in CFD simulations of turbulent flow in rough pipes by considering a half roughness element height blocked flow assumption reported by ANSYS Fluent [24], which is latterly called in this paper as "Temsiriphan's concept" and abbreviated by "TC". From this assumption, he assumed that the linear sublayer starts at the middle of the roughness element. Similar to smooth pipe flow CFD modelling, the proper dimensionless wall distance required for near-wall grid size estimation of rough pipe flow CFD simulation was obtained at the intersection between the linear sublayer and the logarithmic-law layer. The example for investigating this appropriate dimensionless wall distance can be illustrated in Fig. 1. The Fanning friction factors for inflectional and monotonic roughness types were predicted by two-dimensional axisymmetric fully developed pipe

K. Boonsamer, B. Temsiriphan, P. Thongnoi, S. Areerat, E. Bumrungthaichaichan
and S. Wattananusorn,
How can an appropriate CFD model be developed for turbulent flow
in rough pipes?: Evidence from friction factor prediction,
Rev. int. métodos numér. cálc. diseño ing. (2026). Vol.42, (2), 69

flow domains with periodic boundary conditions, a standard k-epsilon model, and different roughness constant (C_s) values. The near-wall grid sizes obtained by dimensionless wall distance values of 5, 10, 15, 30, 50, and TC were employed. The results revealed that the small near-wall grid sizes were improper for Fanning friction factor prediction. Moreover, the high accuracy in Fanning friction factor prediction was achieved by only specific CFD settings depending on operating conditions.
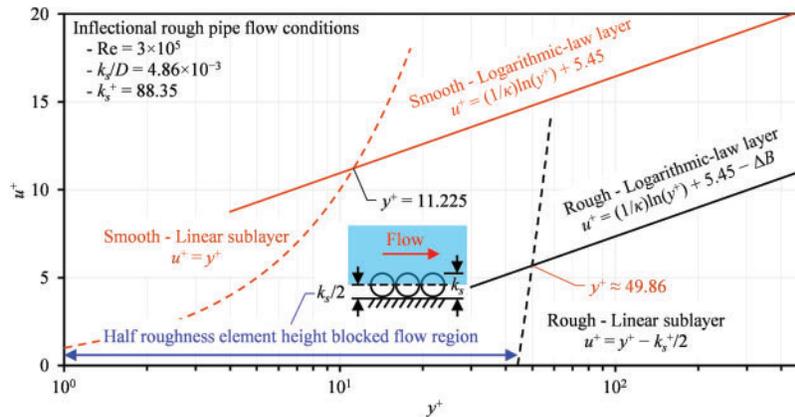

Figure 1: Example for appropriate dimensionless wall distance determination of TC [23]

Boonsamer et al. [25] predicted Fanning friction factors for turbulent inflectional rough pipe flows with Reynolds numbers from 5×10^3 to 5×10^5 by using near-wall grid sizes obtained by dimensionless wall distances of 10, 11.225, 30, TC, and the roughness Reynolds number (k_s^+), or dimensionless roughness height, which is defined as $k_s u_\tau / \nu$ or $\rho k_s u_\tau / \mu$. The two-dimensional axisymmetric CFD models employing the standard k-epsilon model were used to predict developing and fully developed pipe flows as well as Fanning friction factors for a relative roughness (k_s/D) of 0.00486. The results showed that the proper near-wall grid sizes were obtained by the dimensionless wall distance of roughness Reynolds number. Later, Boonsamer [26] extended the inflectional rough surface pipe study by predicting the Fanning friction factors for relative roughness of 0.00105. Moreover, the non-dimensional mean velocity profiles, or near-wall velocity profiles as termed in his work, for both relative roughness values were analyzed and reported in his thesis. The predicted results still confirmed that the appropriate dimensionless wall distance required for estimating the near-wall grid size in turbulent rough pipe flow was the roughness Reynolds number.

At first sight, the information provided by these previous CFD works is seemingly adequate to develop the proper CFD model for turbulent rough pipe flow. Although the proper near-wall grid sizes for inflectional rough pipe flow CFD simulations were successfully investigated by Boonsamer et al. [25] and Boonsamer [26], the appropriate guideline for near-wall grid size estimation for monotonic rough pipe flows was still controversial as previously reported by Temsiriphan [23]. Furthermore, there are several wall roughness treatment approaches. This information indicates that the RANS equation-based CFD modelling for turbulent flow in rough pipes remains a challenging issue for further investigation, especially for monotonic roughness in the transitionally rough regime.

Therefore, in the present work, the near-wall grid sizes were rationally determined by dimensionless wall distances being 11.225, 30, TC, and the roughness Reynolds number to investigate near-wall grid sizes for appropriate CFD modeling of isothermal Newtonian turbulent flows in inflectional and monotonic rough pipes by using the standard k-epsilon model with scalable wall functions. The Fanning friction factors and non-dimensional mean velocity profiles predicted by two different

K. Boonsamer, B. Temsiriphan, P. Thongnoi, S. Areerat, E. Bumrungthaichaichan
and S. Wattananusorn,
How can an appropriate CFD model be developed for turbulent flow
in rough pipes?: Evidence from friction factor prediction,
Rev. int. métodos numér. cálc. diseño ing. (2026). Vol.42, (2), 69

roughness treatment approaches for turbulent flows in 0.246888 m-diameter pipes with inflectional and monotonic rough surfaces were analyzed. It is noted that these two different roughness treatment approaches are described in a later section. The roughness heights of 0.00026 m (relative roughness of 0.00105) and 0.0012 m (relative roughness of 0.00486), which are similar to our previous works [25,26], were studied for both roughness types. The Reynolds numbers of 5×10^4, 1×10^5, 3×10^5, and 5×10^5 were investigated. From these conditions, the studied roughness Reynolds numbers are summarized in Table 1. In this work, for inflectional roughness, the Fanning friction factors predicted by the roughness treatment without the half roughness element height blocked flow assumption for the relative roughness of 0.00486 reported by Boonsamer et al. [25] and the relative roughness of 0.00105 reported by Boonsamer [26] and the non-dimensional mean velocity profiles for these relative roughness values of Boonsamer [26] simulated by the same roughness treatment approach were used for comparison with the present results. Finally, the Fanning friction factors and non-dimensional mean velocity profiles predicted in this study and in the previous works [25,26] were analyzed all at once to finalize the comprehensive conclusion of the present work.

Table 1: Summary of the studied roughness Reynolds numbers

Reynolds number	Roughness Reynolds number			
	Inflectional roughness height		Monotonic roughness height	
	0.00026 m	0.0012 m	0.00026 m	0.0012 m
5×10^4	2.69	14.12	2.89	15.36
1×10^5	5.08	28.83	5.57	30.29
3×10^5	15.09	88.35	16.12	89.94
5×10^5	25.47	147.96	26.63	149.58

2 Roughness Treatment

Generally, for RANS equation-based turbulence models, there are two different wall treatments, i.e., wall function approach (y^+-sensitive wall treatment) and near-wall model approach (y^+-insensitive wall treatment) [24,27]. The wall function approach requires less grids in the near-wall region as compared to another because it uses law of the wall to bridge the viscous-dominated region between wall and turbulent core flow [27]. This advantage of the wall function approach encourages many researchers to develop their turbulent flow CFD models by using wall function-based turbulence models (y^+-sensitive-wall-treatment-based turbulence models), e.g., k-epsilon model, RSM, etc.

For smooth and rough surface walls, the law of the wall for mean velocity can be written in general form as shown in Eq. (2) [24,27].

$$u^+ = \frac{1}{\kappa} \ln y^+ + 5.45 - \Delta B \tag{2}$$

where u^+ is the dimensionless velocity and can be defined as a ratio of mean velocity ($\overline{u}$) to friction velocity. κ is the von Kármán constant, which equals 0.4187. ΔB is the roughness parameter, which is a function of roughness Reynolds number. From the Nikuradse's experimental data [1], Cebeci and Bradshaw [28] gave roughness parameter formulas for hydrodynamically smooth regime ($k_s^+ \leq 2.25$), transitionally rough regime ($2.25 < k_s^+ \leq 90$), and completely rough regime ($k_s^+ > 90$), which were latterly expressed in the compatible forms by ANSYS Fluent as shown in Eqs. (3)–(5) [24], respectively.

K. Boonsamer, B. Temsiriphan, P. Thongnoi, S. Areerat, E. Bumrungthaichaichan
and S. Wattananusorn,
How can an appropriate CFD model be developed for turbulent flow
in rough pipes?: Evidence from friction factor prediction,
Rev. int. métodos numér. cálc. diseño ing. (2026). Vol.42, (2), 69

$$\Delta B = 0 \tag{3}$$

$$\Delta B = \frac{1}{\kappa} \ln \left[\frac{k_s^+ - 2.25}{87.75} + C_s k_s^+ \right] \times \sin \left[0.4258 \left(\ln k_s^+ - 0.811 \right) \right] \tag{4}$$

$$\Delta B = \frac{1}{\kappa} \ln \left(1 + C_s k_s^+ \right) \tag{5}$$

For uniform sand grains, the roughness constant is 0.5, which is a default value for modelling roughness in ANSYS Fluent [24].

As mentioned previously, the present work considered two different roughness treatment approaches. For the first roughness treatment approach, the dimensionless wall distance computed by the normal distance between wall and computing node of the first near-wall cell is directly substituted into Eq. (2) to compute mean velocity. That is the dimensionless wall distance for the mean velocity computation of the wall functions (y_{WF}^+) equals dimensionless wall distance of the first near-wall computing node (y_{NWC}^+). The first roughness treatment approach is now abbreviated by "RT1" to conveniently mention in the latter section. For the second roughness treatment approach, a half roughness element height blocked flow assumption was applied [24]. Therefore, the dimensionless wall distance for the wall functions equals summation of dimensionless wall distance of the first near-wall computing node and half of roughness Reynolds number, i.e., $y_{WF}^+ = y_{NWC}^+ + k_s^+/2$ [24]. In order to conveniently mention the second roughness treatment approach in the latter part of the present work, it is abbreviated by "RT2".

3 CFD Modelling of Turbulent Flow in Rough Pipe

In this work, the present CFD settings were similar to our previous CFD models [25,26] to warrant fair result comparisons. The complete CFD setups of isothermal Newtonian turbulent flows in inflectional and monotonic rough pipes are described as follows:

3.1 Considered Pipes and Their Grid Generation

For all CFD simulations, the 9.72 inch-inner diameter circular pipe, which was experimentally investigated by Laufer [29], was employed similar to our previous CFD works [25,26]. The computational domain of turbulent flow in pipe was simplified by using two-dimensional axisymmetric domain. So, the computational domain width (W) was 0.123444 m, which corresponded to the inner pipe radius (R). To ensure that the fluid flow in the pipe was fully developed, the computational domain length (L) was determined by entry length (L_e) + 20 times pipe diameter, where $L_e = 4.4D \left(\text{Re}^{1/6} \right)$ [30]. Meaning that the computational domain lengths were different depending on Reynolds number. It is noted that although the entry-length correlation used in this work has been confirmed in previous studies [31–33] to achieve fully developed flow in their systems, the computational domain length determined by this correlation was extended by an additional 20 pipe diameters in this work to guarantee that it exceeded the entrance region. Moreover, since the entry length of a rough pipe is shorter than that of a smooth pipe as reported by Li et al. [34], the additional length adopted in the present computational domain is considered sufficient to ensure fully developed flow.

For grid generation, Eq. (1) was computed by using different dimensionless wall distances of 11.225, 30, TC, and the roughness Reynolds number to obtain near-wall grid sizes of turbulent rough pipe flow CFD models. It is noted that the CFD models with near-wall grid sizes obtained by dimensionless wall distances of 11.225, 30, TC, and the roughness Reynolds number are labeled as

K. Boonsamer, B. Temsiriphan, P. Thongnoi, S. Areerat, E. Bumrungthaichaichan
and S. Wattananusorn,
How can an appropriate CFD model be developed for turbulent flow
in rough pipes?: Evidence from friction factor prediction,
Rev. int. métodos numér. cálc. diseño ing. (2026). Vol.42, (2), 69

"NWG1", "NWG2", "NWG3", and "NWG4", respectively, to conveniently refer to these four near-wall grid CFD models, i.e., CFD models with different near-wall grid sizes, in a later section. Although explicit forms and approximations of the friction factor correlation (e.g., the Colebrook–White equation) can be obtained using the Lambert W-function and the Wright ω-function, respectively [35], the implicit Fanning friction factor correlations of Afzal [8] in Eq. (6) and Colebrook–White [4] in Eq. (7) were iteratively computed and used in this study to instantly estimate near-wall grid sizes for inflectional and monotonic rough pipes, respectively, and to compare with the simulated results.

$$\frac{1}{\sqrt{f_F}} = -4\log_{10}\left[\frac{k_s/D}{3.7}\exp\left\{-j\frac{1.415}{\mathrm{Re}\,(k_s/D)\,\sqrt{f_F}}\right\} + \frac{1.255}{\mathrm{Re}\sqrt{f_F}}\right] \tag{6}$$

$$\frac{1}{\sqrt{f_F}} = -4\log_{10}\left[\frac{k_s/D}{3.7} + \frac{1.255}{\mathrm{Re}\sqrt{f_F}}\right] \tag{7}$$

For Eq. (6), j is 11 for inflectional roughness and 0 for monotonic roughness (when j equals 0, the Afzal correlation [8] reduces to the Colebrook-White equation [4]). The near-wall grid sizes of the present turbulent rough pipe flow CFD models are summarized in Table 2. Quadrilateral grid cells were generated inside the two-dimensional computational domains to minimize numerical errors [36]. The growth ratio in radial was 1.05–1.07 (starting from the wall towards the pipe center) depending on near-wall grid size [25,26]. For axial direction, the grid generation was distinguished into 2 zones, i.e., a gradually distributed grid zone and equilateral grid length zone. Regarding the first 35 grid layers beyond the inlet, grids underwent expansion with the growth ratio of 1.1 [25,26]. In the equilateral grid length zone, the uniform grid lengths were applied. Moreover, in the second zone, the near-wall grid aspect ratios were controlled to not exceed the maximum value of 100 typically allowed in the boundary layer [37], with values ranging from 38.3 to 38.7. The schematic of pipe flow domain and example of grid generation for two-dimensional pipe flow domain are illustrated in Fig. 2.

Table 2: Summary of near-wall grid sizes for the present turbulent rough pipe flow CFD models

Reynolds number	CFD model	Target y^+ for near-wall grid size estimation	Near-wall grid size [mm]			
			Inflectional roughness height		Monotonic roughness height	
			0.00026 m	0.0012 m	0.00026 m	0.0012 m
5×10^4	NWG1	11.225	2.1660	1.9075	2.0174	1.7542
	NWG2	30	5.7888	5.0980	5.3916	4.6882
	NWG3	TC	2.4468	2.8685	2.3030	2.7098
	NWG4	Roughness Reynolds number	0.5182	2.4000	0.5182	2.4000
1×10^5	NWG1	11.225	1.1492	0.9345	1.0488	0.8895
	NWG2	30	3.0713	2.4974	2.8029	2.3772
	NWG3	TC	1.4134	1.9073	1.3057	1.8665
	NWG4	Roughness Reynolds number	0.5182	2.4000	0.5182	2.4000

(Continued)

K. Boonsamer, B. Temsiriphan, P. Thongnoi, S. Areerat, E. Bumrungthaichaichan
and S. Wattananusorn,
How can an appropriate CFD model be developed for turbulent flow
in rough pipes?: Evidence from friction factor prediction,
Rev. int. métodos numér. cálc. diseño ing. (2026). Vol.42, (2), 69

Table 2 (continued)

| Reynolds number	CFD model	Target y^+ for near-wall grid size estimation	Near-wall grid size [mm]			
			Inflectional roughness height		Monotonic roughness height	
			0.00026 m	0.0012 m	0.00026 m	0.0012 m
3×10^5	NWG1	11.225	0.3870	0.3050	0.3623	0.2996
	NWG2	30	1.0343	0.8150	0.9683	0.8006
	NWG3	TC	0.5936	1.3958	0.5682	1.3922
	NWG4	Roughness Reynolds number	0.5182	2.4000	0.5182	2.4000
5×10^5	NWG1	11.225	0.2293	0.1821	0.2193	0.1801
	NWG2	30	0.6129	0.4867	0.5860	0.4814
	NWG3	TC	0.4373	1.3146	0.4279	1.3133
	NWG4	Roughness Reynolds number	0.5182	2.4000	0.5182	2.4000
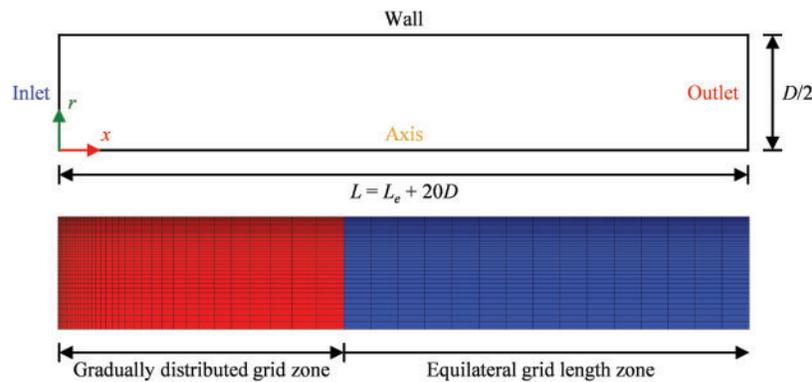
Figure 2: Schematic of computational pipe flow domain and example of grid generation

3.2 Physical Settings

The mean flow and turbulence fields for air flow in rough pipes were resolved by steady state RANS equations with the standard k-epsilon model and scalable wall-functions. See also ANSYS Fluent theory guide [27] for the complete details of these transport equations. The density and viscosity of air were 1.229 kg·m^{-3} and 1.73×10^{-5} Pa·s, respectively.

At the inlet, the velocity-inlet boundary condition type was used. The uniform inlet velocities of 2.8508, 5.702, 17.105, and 28.508 m·s^{-1} were specified for Reynolds numbers of 5×10^4, 1×10^5, 3×10^5, and 5×10^5, respectively. For turbulence at the inlet, turbulence intensity (I) computed by $0.16Re^{-1/8}$ and hydraulic diameter of 0.246888 m were imposed. At the outlet, the zero gauge pressure was set for pressure-outlet boundary condition type. The outlet turbulence specifications were

K. Boonsamer, B. Temsiriphan, P. Thongnoi, S. Areerat, E. Bumrungthaichaichan
and S. Wattananusorn,
How can an appropriate CFD model be developed for turbulent flow
in rough pipes?: Evidence from friction factor prediction,
Rev. int. métodos numér. cálc. diseño ing. (2026). Vol.42, (2), 69

identical to those of inlet. At the pipe wall, no-slip boundary condition was used. For two-dimensional axisymmetric computational domain, the axis boundary condition type was applied at the domain axis.

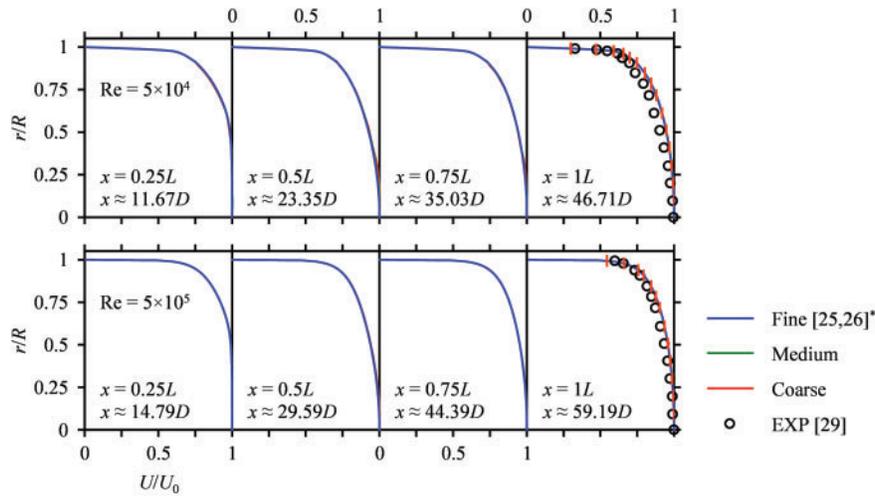### 3.3 Numerical Settings and Solution Strategy

In the present work, the steady state double precision pressure-based solver was used. The SIMPLE was employed for pressure-velocity coupling algorithm. The discretization schemes for gradient and pressure were least squares cell based and second order, respectively. Furthermore, the discretization schemes of momentum, turbulence kinetic energy (k or TKE), and turbulence dissipation rate (ε or TDR) were second order upwind.

The scaled residuals of all transport equations were monitored to identify solution convergence. The simulations were performed until all scaled residuals were constant or slightly different to warrant solution and iterative convergences [38].

3.4 Grid Independent Solutions

Although our previous works [25,26] have already confirmed grid independent solutions for the CFD simulation of turbulent pipe flow at a Reynolds number of 5×10^5, the three grid resolutions differed significantly only in the radial direction, with a refinement factor of approximately 1.2. Therefore, in the present work, the grid independent solutions for pipe flow with Reynolds numbers of 5×10^4 and 5×10^5 were re-analyzed by comparing the profiles of normalized mean axial velocity, which can be defined as a ratio of mean axial velocity (U) to centerline axial velocity (U_0), obtained by fine grid resolution cases of our previous works [25,26] with those simulated by medium and coarse grid levels of the present work as shown in Fig. 3. It is noted that, unlike in the previous works [25,26], both node and cell-center values were adopted for plotting the normalized mean axial velocity profiles in Fig. 3 to minimize the error caused by interpolation of the plotting software. Moreover, the grid convergence index (GCI) analysis for Fanning friction factors of these two different Reynolds numbers was assessed to quantitatively obtain grid convergence by following the comprehensive GCI procedure suggested by Bumrungthaichaichan et al. [39] as reported in Table 3.

From Fig. 3, the radial profiles of normalized mean axial velocity in developing ($x = 0.25\ L$ and $0.5\ L$) and fully developed ($x = 0.75\ L$ and $1\ L$) zones for two different Reynolds numbers predicted by three different grid resolutions are insignificantly different. From GCI analysis reported in Table 3, convergence ratios of -0.1061 for Reynolds number of 5×10^4 and 0.7102 for Reynolds number of 5×10^5 indicate oscillatory and monotonic convergence, respectively. The α values for two different Reynolds numbers are approximately one, which mean that the Fanning friction factors predicted by grid refinement from coarse to fine grid resolutions are in asymptotic range. For GCI comparisons, $\text{GCI}_{21} < \text{GCI}_{32}$ confirms grid independent solutions for two different simulations. Moreover, the error bars on normalized mean axial velocity profiles were obtained by average apparent order of discretization method of 5.21 for Reynolds number of 5×10^4 and 18.19 for Reynolds number of 5×10^5. The maximum discretization uncertainties for these Reynolds numbers were lower than 1%. Although these results reveal that coarse grid resolution is adequate to obtain grid independence, the fine grid qualities were adopted for developing the present CFD models for turbulent flows in rough pipes to minimize any numerical uncertainties.

K. Boonsamer, B. Temsiriphan, P. Thongnoi, S. Areerat, E. Bumrungthaichaichan
and S. Wattananusorn,
How can an appropriate CFD model be developed for turbulent flow
in rough pipes?: Evidence from friction factor prediction,
Rev. int. métodos numér. cálc. diseño ing. (2026). Vol.42, (2), 69

Figure 3: Radial profiles of normalized mean axial velocity for Reynolds number of 5×10^4 and 5×10^5 at x/L of 0.25, 0.5, 0.75, and 1 predicted by three different grid resolutions

Table 3: GCI analysis for Fanning friction factor

Reynolds number	i^1	N_i	f_i (Fanning friction factor)	% Difference^2	$r_{i+1,i}$	p^3	GCI [%]	R^4	α^5
5×10^4	0^6	–	4.8980×10^{-3}						
	1	1064	4.8979×10^{-3}	–					
					1.2602		0.0034		
	2	670	4.8968×10^{-3}	0.0224		9.6154		−0.1061	1.0045
					1.2630		0.0313		
	3	420	4.9072×10^{-3}	0.1890					
5×10^5	0^6	–	3.1427×10^{-3}						
	1	21,320	3.1344×10^{-3}	–					
					1.3185		0.3287		
	2	12,264	3.1312×10^{-3}	0.1021		1.1864		0.7102	0.9990
					1.3226		0.4568		
	3	7011	3.1267×10^{-3}	0.2457					

Notes: $^1 i = 0$, 1, 2, and 3 denote zero grid space, fine grid level, medium grid level, and coarse grid level, respectively; ^{2}The percentage difference is defined as $\left(\left| f_{F,CFD} - f_{F,Fine} \right| / f_{F,Fine} \right) \times 100$; $^3 p$ is the apparent order of discretization method; $^4 R$ is the convergence ratio (monotonic convergence for $0 < R < 1$, oscillatory convergence for $R < 0$, and divergence for $R > 1$) and can be computed by e_{21}/e_{32}, where $e_{i+1,i} = (f_{i+1} - f_i)/f_i$; $^5 \alpha$ is the variable for asymptotic range of convergence identification and can be calculated by $\left((r_{21})^p \text{ GCI}_{21} \right) / \text{GCI}_{32}$; ^{6}For $i = 0$, the value at zero grid space (f_0) is obtained by Richardson extrapolation as $f_0 = f_1 + (f_1 - f_2)/\left((r_{21})^p - 1 \right)$.

3.5 Model Validation

For model validation, the predicted fully developed normalized mean axial velocity profiles at the outlet were compared to the measured fully developed velocity profiles of Laufer [29] as depicted in Fig. 3. Fig. 3 reveals that the predicted profiles for Reynolds numbers of 5×10^4 and 5×10^5 slightly

K. Boonsamer, B. Temsiriphan, P. Thongnoi, S. Areerat, E. Bumrungthaichaichan
and S. Wattananusorn,
How can an appropriate CFD model be developed for turbulent flow
in rough pipes?: Evidence from friction factor prediction,
Rev. int. métodos numér. cálc. diseño ing. (2026). Vol.42, (2), 69

deviate from the previous experimental data reported by Laufer [29]. Due to the information loss inherent in the time-averaging process [40,41] of the RANS equations, a perfect match between the results of RANS equation-based CFD models and measured data is rarely obtained. This limitation contributed to the observed discrepancies in the normalized mean axial velocity profiles. Moreover, the differences in upstream conditions for the present CFD simulations (uniform velocity profile) and experiment of Laufer [29] (velocity profile induced by sandpaper-accelerated boundary layer growth) can also result in deviations due to the memory effect [42], which resulting in a delayed response to disturbances. Therefore, based on these comparisons and explanations, it can be summarized that the present CFD models are reasonable for predicting turbulent pipe flows.

4 Results and Discussion

In the present work, the predicted Fanning friction factors for different conditions were compared to those obtained by correlations [4,8] to investigate the proper near-wall grid size and roughness treatment approach for simulating turbulent flows in inflectional and monotonic rough pipes as reported in Section 4.1. Moreover, the predicted non-dimensional mean velocity profiles were compared to the rough wall logarithmic-law profiles for rough surface to achieve the proper CFD models for turbulent rough pipe flows as shown in Section 4.2. It is noted that, for NWG4s, the results for inflectional roughness predicted by RT1 from our previous works [25,26] and by RT2 in the present work, both with a roughness constant of 0.5, were used for monotonic roughness under the same Reynolds number and relative roughness throughout this work due to the identical CFD simulation.

4.1 Fanning Friction Factor

For inflectional roughness, the Fanning friction factors predicted by two roughness treatment approaches with roughness constant of 0.5 for different Reynolds numbers, relative roughness values, and near-wall grid CFD models were compared to those computed by Afzal correlation [8] as shown in Fig. 4. According to the previous work of Temsiriphan [23], his simulated results showed that the higher roughness constant was suitable for predicting Fanning friction factors of monotonic roughness. Therefore, in the present work, the Fanning friction factors for monotonic roughness predicted by roughness constants of 0.5 and 0.7 were compared to Fanning friction factors obtained by Colebrook-White correlation [4] as depicted in Figs. 5 and 6, respectively.

Fig. 4 reveals that the Fanning friction factors predicted by NWG4s, near-wall grid sizes obtained by roughness Reynolds number, for two roughness treatment approaches are in better agreement with those of the Afzal correlation [8] under all studied conditions than other models. For RT1, NWG4s yield the highest Fanning friction factors, while both larger and smaller near-wall grid sizes result in lower values. For example, at a Reynolds number of 3×10^5, the Fanning friction factor for a relative roughness of 0.00105 predicted by NWG4 (0.5182 mm) is 0.004597. For the smaller near-wall grid size of NWG1 (0.3870 mm) and the larger near-wall grid sizes of NWG3 (0.5936 mm) and NWG 2 (1.0343 mm), the Fanning friction factors under the same conditions are 0.004287, 0.004579, and 0.004528, respectively. However, for the Fanning friction factor prediction of RT2, it can be observed that the larger the near-wall grid size, the lower the Fanning friction factor. That is the Fanning friction factors for a Reynolds number of 3×10^5 and a relative roughness of 0.00105 predicted by RT2 for NWG1, NWG4, NWG3, and NWG2 (ranked from smallest to largest near-wall grid size) are 0.004722, 0.004676, 0.004655, and 0.004584, respectively.
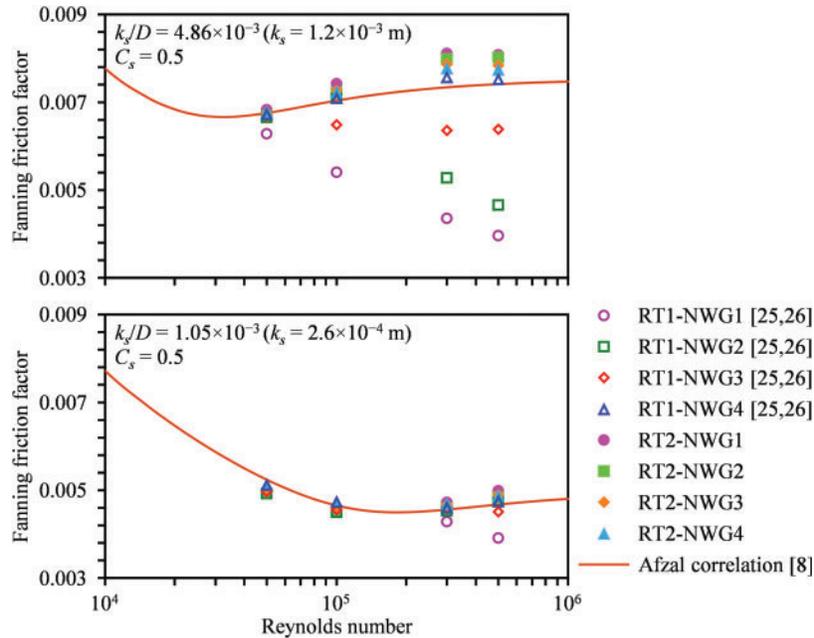
K. Boonsamer, B. Temsiriphan, P. Thongnoi, S. Areerat, E. Bumrungthaichaichan
and S. Wattananusorn,
How can an appropriate CFD model be developed for turbulent flow
in rough pipes?: Evidence from friction factor prediction,
Rev. int. métodos numér. cálc. diseño ing. (2026). Vol.42, (2), 69

Figure 4: Fanning friction factors of inflectional roughness predicted by different near-wall grid CFD models and roughness treatment approaches with roughness constant of 0.5
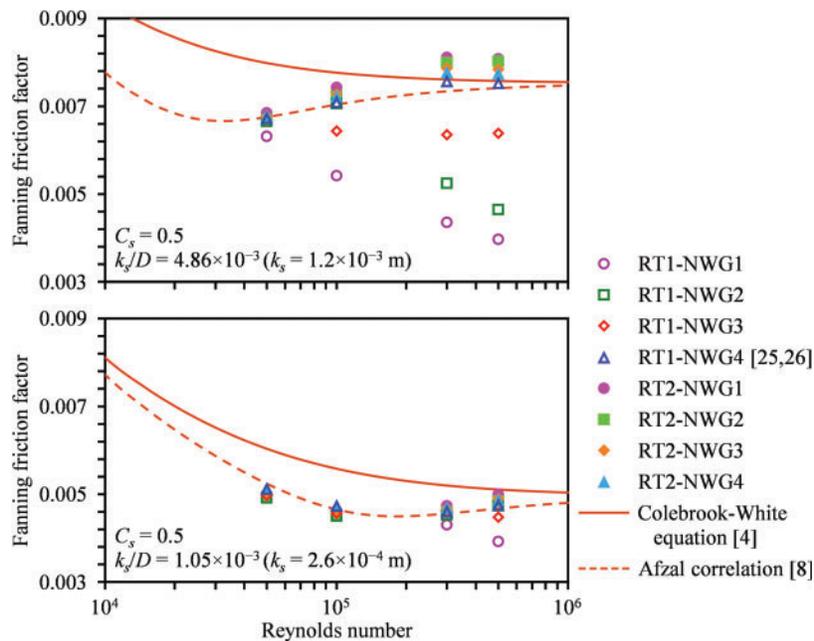

Figure 5: Fanning friction factors of monotonic roughness predicted by different near-wall grid CFD models and roughness treatment approaches with roughness constant of 0.5
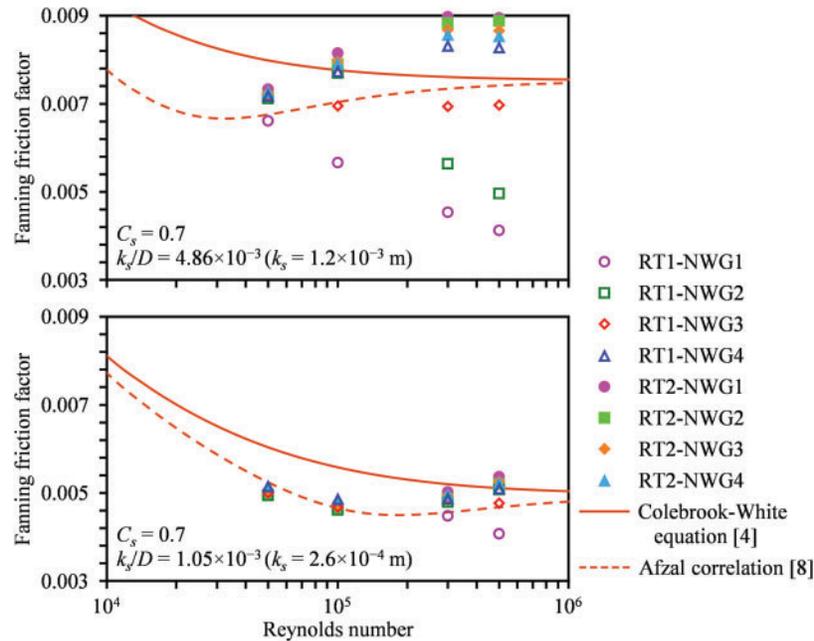
K. Boonsamer, B. Temsiriphan, P. Thongnoi, S. Areerat, E. Bumrungthaichaichan
and S. Wattananusorn,
How can an appropriate CFD model be developed for turbulent flow
in rough pipes?: Evidence from friction factor prediction,
Rev. int. métodos numér. cálc. diseño ing. (2026). Vol.42, (2), 69

Figure 6: Fanning friction factors of monotonic roughness predicted by different near-wall grid CFD models and roughness treatment approaches with roughness constant of 0.7

As shown in Figs. 5 and 6, although the near-wall grid sizes were computed by Colebrook-White equation [4] for monotonic roughness, the Fanning friction factors predicted by roughness constants of 0.5 and 0.7 still follow inflectional roughness cases because the employed wall functions were developed based on Nikuradse's experimental data for sand grain (inflectional) roughness [1]. It is worth reiterating that the results for the inflectional roughness predicted by NWG4s with RT1 and a roughness constant of 0.5 in our previous works [25,26] were used for the monotonic roughness in Fig. 5 and elsewhere in this work because both roughness types employed an identical CFD model under the same Reynolds number and relative roughness. The trends of the Fanning friction factors predicted by four different near-wall grid CFD models for RT1 and RT2 are similar to those of inflectional roughness as previously described. Moreover, a roughness constant of 0.7 predicts Fanning friction factors approximately 0.5% to 11% higher than those with 0.5, depending on the tested conditions. Increasing the roughness constant from 0.5 to 0.7 can both improve and deteriorate the accuracy of the predicted Fanning friction factors.

For relative roughness of 0.00486, the Fanning friction factors predicted by NWG4s at Reynolds numbers of 3×10^5 and 5×10^5, corresponding to roughness Reynolds numbers of 89.94 and 149.58, respectively, for both roughness treatment approaches (roughness constant of 0.5) closely match the values computed by Colebrook-White equation [4] as shown in Fig. 5, similar to the results of inflectional rough pipe CFD simulations. Unsurprisingly, although the present CFD models were developed by inflectional roughness-based wall functions, they effectively predicted monotonic friction factors in near-completely rough and completely rough regimes. This is because at high Reynolds numbers in completely rough regime, the inertial force dominates the flow and friction factors depend mainly on roughness height rather than on roughness shape, spacing, and uniformity [1,4–6]. In other words, the effects of roughness shape, spacing, and uniformity are overshadowed by the roughness height.

K. Boonsamer, B. Temsiriphan, P. Thongnoi, S. Areerat, E. Bumrungthaichaichan
and S. Wattananusorn,
How can an appropriate CFD model be developed for turbulent flow
in rough pipes?: Evidence from friction factor prediction,
Rev. int. métodos numér. cálc. diseño ing. (2026). Vol.42, (2), 69

On the other hand, as the Reynolds number decreases from the completely rough to the transitionally rough regime, the influence of roughness height weakens, while the roughness uniformity becomes increasingly important in shaping flow dynamics and drag behavior [43–45]. This is a reason why Fanning friction factors at Reynolds numbers of 1×10^5 for a relative roughness of 0.00486 (roughness Reynolds number of 30.29) and 5×10^5 for a relative roughness of 0.00105 (roughness Reynolds number of 26.63) predicted by NWG4s and both roughness treatment approaches with a roughness constant of 0.7 represent good agreement with those of Colebrook-White equation [4] as depicted in Fig. 6. These predicted results are consistent with the recommendation of ANSYS Fluent that the roughness constant for non-uniform roughness ranges from 0.5 to 1.0 [24]. Generally, at the same Reynolds number, the Fanning friction factor increases with increasing roughness height or with greater surface roughness non-uniformity, particularly in the transitionally rough regime, whereas it decreases when these parameters are reduced [6]. Moreover, Eqs. (4) and (5) indicate that increasing the roughness Reynolds number and/or roughness constant leads to an increase in ΔB, and *vice versa*, meaning both parameters affect ΔB in the same manner. This implies that an increase in the roughness constant also results in a higher predicted Fanning friction factor, explaining why a higher roughness constant is required to predict the Fanning friction factor of monotonic (more non-uniform) roughness. Nevertheless, since a universally accepted criterion for specifying roughness constant for arbitrary surface types is unavailable [24], a roughness constant of 0.7 suggested by Temsiriphan [23] was adopted for modelling monotonic roughness type in the present study. Even with this value (roughness constant of 0.7), noticeable discrepancies in Fanning friction factor prediction persist for roughness Reynolds numbers below 26.63 as shown in Fig. 6.

Generally, for RANS turbulence model-based CFD simulation with wall functions, the prediction accuracy depends mainly on both near-wall and core flow calculations. From the predicted Fanning friction factors shown in Fig. 6, increasing the roughness constant can possibly improve the accuracy of Fanning friction factor predictions for monotonic roughness from the middle toward the lower end of the transitionally rough regime. Moreover, at the same Reynolds number within the lower end of the transitionally rough regime, the greater asymmetry induced by non-uniform roughness leads to higher entropy generation, resulting in an increase in turbulence kinetic energy production [46]. Therefore, in order to obtain more accurate predicted Fanning friction factors for roughness Reynolds numbers below 26.63, higher roughness constant was employed to simulate monotonic roughness pipe flow in the near-wall region. Furthermore, in the core flow region, the turbulence model constant C_μ, hereafter simply referred to as "turbulence model constant", was increased to gain more turbulence kinetic energy production in monotonic roughness pipe flow with lower roughness Reynolds numbers. The Fanning friction factors predicted by the appropriately higher roughness and turbulence model constants are represented in Fig. 7.

In Fig. 7, the results reveal that the application of the appropriate higher roughness and turbulence model constants successfully predicts the Fanning friction factors for lower roughness Reynolds numbers of monotonic roughness pipes. These successful CFD simulations inform that for monotonic roughness, the lower the roughness Reynolds number, the higher the roughness and turbulence model constants. Moreover, the Fanning friction factors for lower roughness Reynolds numbers of monotonic roughness pipe predicted by NWG4s developed by two different roughness treatment approaches with the appropriate roughness and turbulence model constants show better agreement with those calculated by Colebrook-White equation [4] than other models. Different roughness and turbulence model constants were employed to accurately predict the Fanning friction factors of monotonic roughness in the middle to the lower end of transitionally rough regime. This is because the discrepancy in the friction factor between inflectional and monotonic roughness types (i.e., between more uniform

K. Boonsamer, B. Temsiriphan, P. Thongnoi, S. Areerat, E. Bumrungthaichaichan
and S. Wattananusorn,
How can an appropriate CFD model be developed for turbulent flow
in rough pipes?: Evidence from friction factor prediction,
Rev. int. métodos numér. cálc. diseño ing. (2026). Vol.42, (2), 69

and more non-uniform roughness types) varies with the roughness Reynolds number [47–49], as interpreted from the differences between the Nikuradse and Colebrook roughness functions.
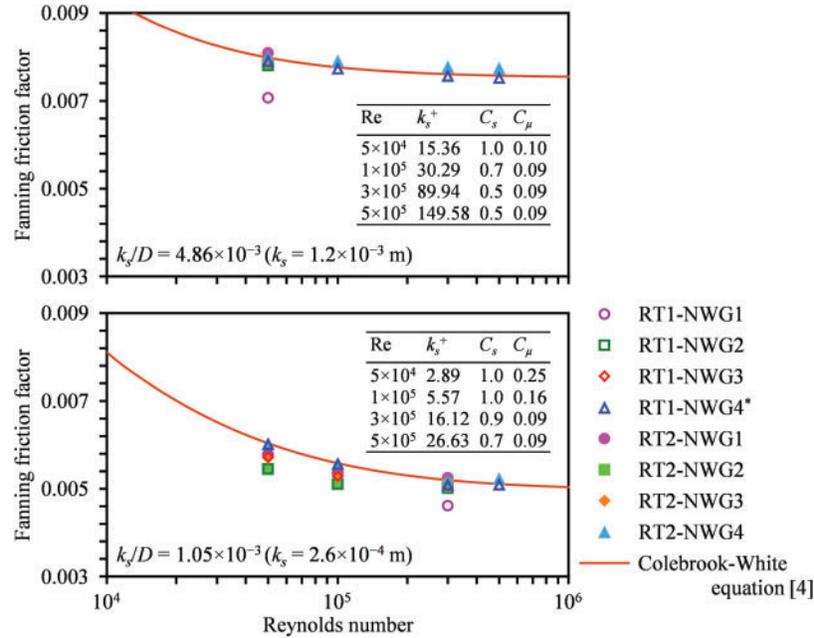
Figure 7: Fanning friction factors of monotonic roughness predicted by different near-wall grid CFD models and roughness treatment approaches with appropriate roughness and turbulence model constants

After demonstrating that the adjusted roughness and turbulence model constants yield more accurate predictions of the Fanning friction factor for monotonic roughness, only a representative case with roughness constant increased from 0.5 to 1.0 and turbulence model constant increased from 0.09 to 0.25 is presented to elucidate the associated turbulence parameters at the lower end of the transitionally rough regime. The profiles of turbulence viscosity ratio ($\mu_t^+ \equiv \mu_t/\mu$ where μ_t is the turbulence viscosity.), inner-scaled turbulence kinetic energy production ($P_k^+ \equiv P_k \nu/u_\tau^4$), inner-scaled turbulence dissipation rate ($\varepsilon^+ \equiv \varepsilon \nu/u_\tau^4$), and inner-scaled turbulence kinetic energy ($k^+ \equiv k/u_\tau^2$) for a relative roughness of 0.00105 at Reynolds number of 5×10^4 predicted by NWG4s developed by two different roughness treatment approaches with appropriate settings for inflectional and monotonic roughness types were compared as shown in Fig. 8. It is noted that the friction velocity for inflectional (uniform) roughness was used in the present work to normalize the turbulence quantities and to obtain dimensionless wall distance.
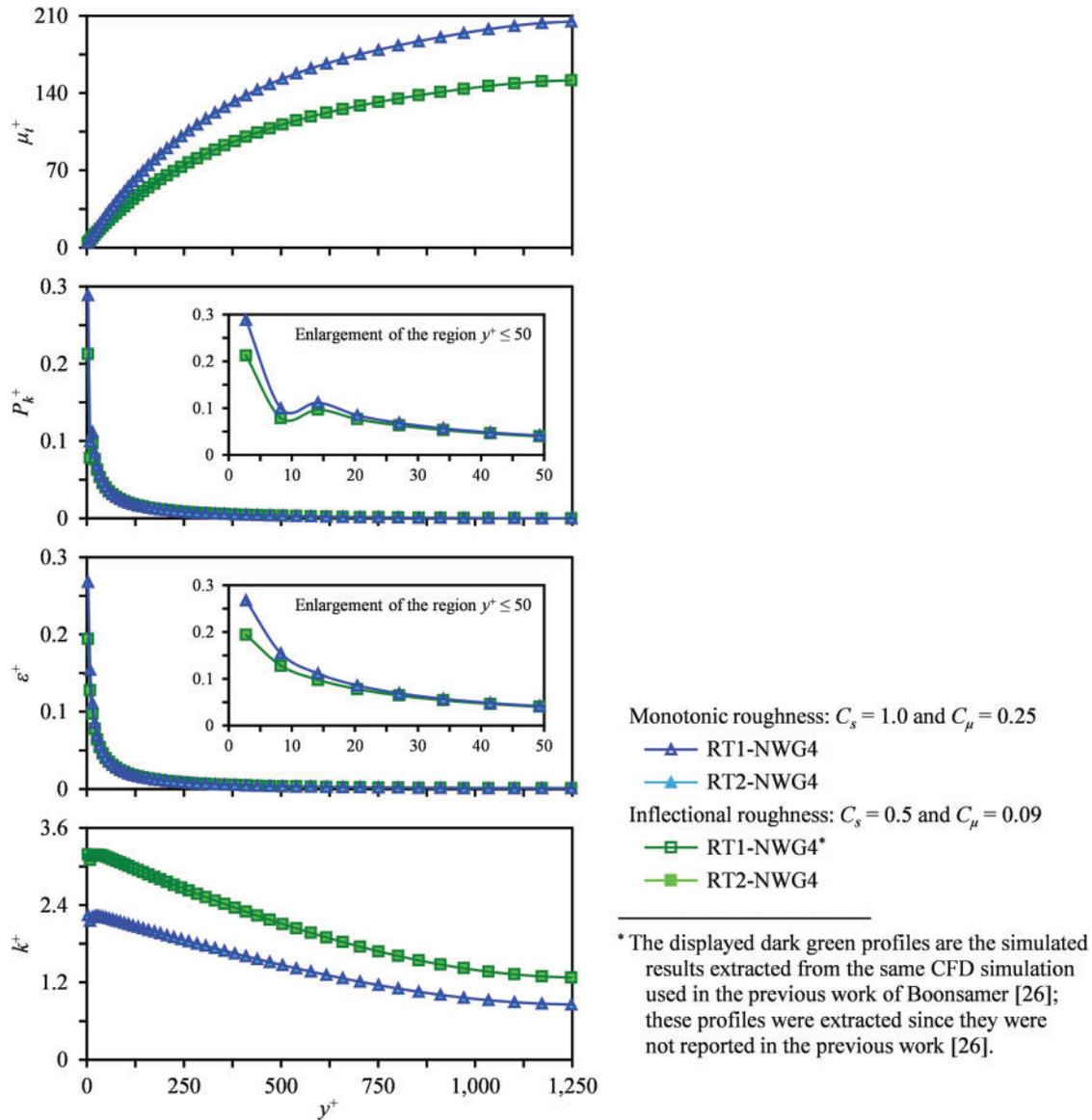
K. Boonsamer, B. Temsiriphan, P. Thongnoi, S. Areerat, E. Bumrungthaichaichan
and S. Wattananusorn,
How can an appropriate CFD model be developed for turbulent flow
in rough pipes?: Evidence from friction factor prediction,
Rev. int. métodos numér. cálc. diseño ing. (2026). Vol.42, (2), 69

Figure 8: Turbulence viscosity ratio, inner-scaled turbulence kinetic energy production, inner-scaled turbulence dissipation rate, and inner-scaled turbulence kinetic energy profiles of inflectional and monotonic roughness types for a relative roughness of 0.00105 at Reynolds number of 5×10^4 predicted by NWG4s developed by two different roughness treatment approaches with appropriate roughness and turbulence model constants

Fig. 8 reveals that increasing the turbulence model constant from 0.09 to 0.25 for monotonic (non-uniform) roughness enhances the turbulence viscosity, resulting in increased turbulence kinetic energy production and turbulence dissipation rate, especially in the near-wall region. In contrast, due to enhanced turbulence diffusion and dissipation, the turbulence kinetic energy levels for monotonic roughness are decreased, which similar to the previous direct numerical simulation (DNS) results for idealized and irregular rough surfaces of Bhaganagar and Chau [50] that predicted turbulence

K. Boonsamer, B. Temsiriphan, P. Thongnoi, S. Areerat, E. Bumrungthaichaichan
and S. Wattananusorn,
How can an appropriate CFD model be developed for turbulent flow
in rough pipes?: Evidence from friction factor prediction,
Rev. int. métodos numér. cálc. diseño ing. (2026). Vol.42, (2), 69

intensities for irregular rough surface were lower than those of idealized rough surface. Within each roughness type (inflectional and monotonic), the results predicted by two different roughness treatment approaches are identical. To interpret the turbulence behavior observed in the representative case, plausible physical mechanisms associated with transitionally rough flow can be described below.

In the transitionally rough regime, fluid flow behavior depends strongly on the roughness type [44]. In this regime, non-uniform roughness may produce stronger turbulence production than uniform roughness, as inferred from theoretical work of Wattananusorn [46] and from DNS-predicted turbulence intensity comparisons between random roughness and smooth surfaces [51]. However, the generated turbulence is fragmented and rapidly dissipated because viscous effects remain important, especially in the lower end of the transitionally rough regime, to suppress coherent wake formation for non-uniform rough surface flows, preventing an increase in the mean turbulence kinetic energy; consequently, lower turbulence kinetic energy levels are observed, consistent with the previous DNS work of Bhaganagar and Chau [50], as interpreted from predicted turbulence intensity comparisons between idealized and irregular rough surfaces. In other words, roughness effects in the transitionally rough regime are strongly dependent on roughness morphology and do not necessarily lead to monotonic increases in turbulence kinetic energy. In contrast, uniform roughness may promote more coherent and persistent wake structures, which can enhance turbulence kinetic energy levels. Therefore, non-uniform roughness, referred to as monotonic roughness in this work, can exhibit a higher friction factor while maintaining lower mean turbulence kinetic energy levels, because form drag and mean momentum loss increase due to pressure losses associated with irregular protrusions, even when large coherent wakes are absent. From this explanation, it can be summarized that increasing the roughness constant (0.5–1.0) enhances the model's representation of form drag [43], resulting in a higher friction factor for monotonic roughness within the transitionally rough regime. An increase in the turbulence model constant (>0.09) strengthens the momentum flux toward the wall, steepening the near-wall velocity gradient and thereby increasing the wall shear stress, i.e., yields a higher friction factor for monotonic roughness at the lower end of the transitionally rough regime. Nevertheless, increasing the turbulence model constant enhances the turbulence dissipation rate, thereby reducing turbulence kinetic energy levels. It is emphasized that the mechanisms discussed above are not universal and may vary with roughness morphology and flow conditions, reflecting the inherent complexity of rough-surface turbulent flows.

In addition, the normalized mean square error (NMSE) values for Fanning friction factors predicted by four different grid models were computed and compared to indicate the appropriate turbulent rough pipe flow CFD model as reported in Table 4. From the previous CFD studies [52–54], NMSE can be determined by $\sum_{i=1}^{n} (O_i - P_i)^2 / \sum_{i=1}^{n} (O_i P_i)$, where O_i and P_i are reference and predicted values for each tested condition, respectively.

From Table 4, NWG4s represent the lowest NMSE values for all conditions. Generally, the lower NMSE value indicates higher prediction accuracy. Hence, these results confirm that NWG4 is appropriate for predicting Fanning friction factors of turbulent rough pipe flows. That is the near-wall grid sizes for turbulent rough pipe flow CFD models should be obtained by dimensionless wall distance of roughness Reynolds number. In other words, the near-wall grid sizes for vertex-based and cell-center-based CFD codes are roughness height and twice the roughness height, respectively.

K. Boonsamer, B. Temsiriphan, P. Thongnoi, S. Areerat, E. Bumrungthaichaichan
and S. Wattananusorn,
How can an appropriate CFD model be developed for turbulent flow
in rough pipes?: Evidence from friction factor prediction,
Rev. int. métodos numér. cálc. diseño ing. (2026). Vol.42, (2), 69

Table 4: Normalized mean square error for Fanning friction factors predicted by different near-wall grid CFD models and roughness treatment approaches

CFD model	NMSE								
	Inflectional			Monotonic			Both roughness types		
	RT1	RT2	Overall	RT1	RT2	Overall	RT1	RT2	Overall
NWG1	0.1076	0.0044	0.0481	0.1113	0.0023	0.0486	0.1097	0.0033	0.0483
NWG2	0.0465	0.0032	0.0231	0.0478	0.0027	0.0236	0.0472	0.0029	0.0234
NWG3	0.0089	0.0021	0.0053	0.0122	0.0011	0.0064	0.0107	0.0015	0.0059
NWG4	0.0003	0.0013	0.0008	0.0001	0.0002	0.0001	0.0002	0.0007	0.0004

According to the predicted Fanning friction factors, it can be summarized that the NWG4s with the appropriate roughness and turbulence model constants provide good agreement with the correlations [4,8] in predicting Fanning friction factors for both inflectional and monotonic roughness types, regardless of roughness treatment approach. For inflectional roughness, a roughness constant of 0.5 is appropriate to accurately predict the Fanning friction factors under all studied conditions. This CFD model can also be adopted to predict Fanning friction factors for monotonic roughness in the near-completely rough and completely rough regimes. From the upper to lower end of the transitionally rough regime, the higher roughness constant is recommended for accurately predicting Fanning friction factors of monotonic roughness. In addition, the higher turbulence model constant is required to accurately predict Fanning friction factors of monotonic roughness in the middle to lower end of the transitionally rough regime.

4.2 Non-Dimensional Mean Velocity Profile

In this sub-section, the non-dimensional mean velocity profiles precited by two roughness treatment approaches with appropriate roughness and turbulence model constants for inflectional and monotonic roughness types were compared to the rough wall logarithmic-law profiles obtained by Eq. (2) with Eq. (4) or Eq. (5) as shown in Figs. 9 and 10, respectively. It is noted that the term "non-dimensional mean velocity profile" used in the present work refers to the rough-wall mean velocity profile as termed by Schultz and Flack [48]; hereafter, the term "rough wall logarithmic-law profile" denotes the profile obtained by Eq. (2) with Eq. (4) or Eq. (5).

For the logarithmic region, the lower and upper bounds are still controversy [55]. In other words, the boundaries have been specified differently depending on the interpretations of individual researchers [56–58]. Based on the work of Brereton et al. [57], the roughness sublayer extends from the roughness trough to just beyond the roughness crest. From this information, in the present work, the lower limit of the logarithmic region was defined to begin at the roughness height corresponding to the roughness Reynolds number. For the upper limit of the logarithmic region used in this work, the dimensionless wall distance was set to 0.15 of the friction Reynolds number (Re_τ) [56,58]. It is noted that the friction Reynolds number is generally defined as $\delta u_\tau / \nu = \rho \delta u_\tau / \mu$, where δ is the boundary layer thickness or pipe radius or channel half-height [56]. That is for pipe flows, $Re_\tau = R u_\tau / \nu = \rho R u_\tau / \mu$. Therefore, vertical dashed crimson red lines are drawn in Figs. 9 and 10 to illustrate the logarithmic region specified in the present work ($k_s^+ < y^+ < 0.15 Re_\tau$), where the profiles obtained by CFD simulations and correlations were compared.
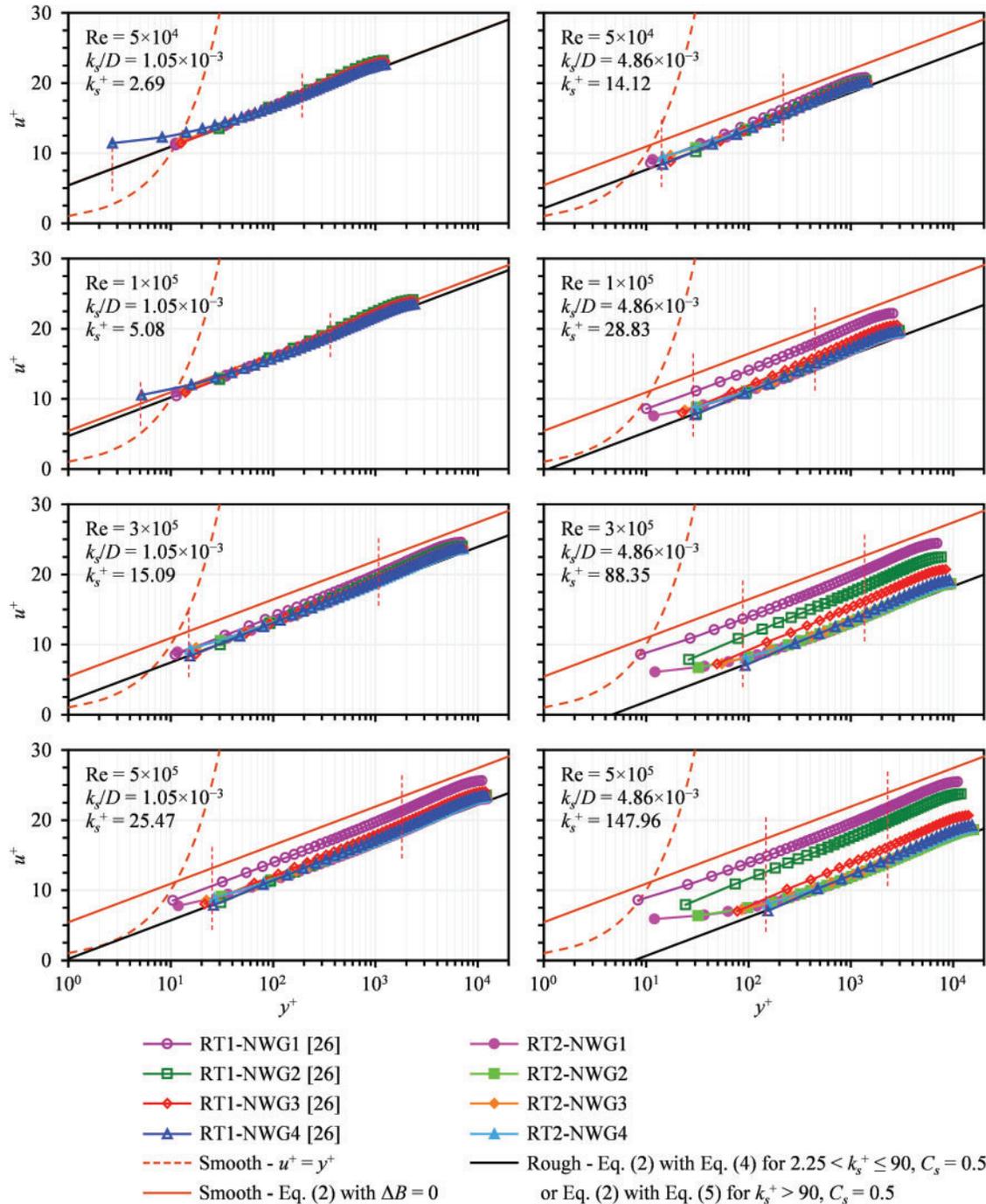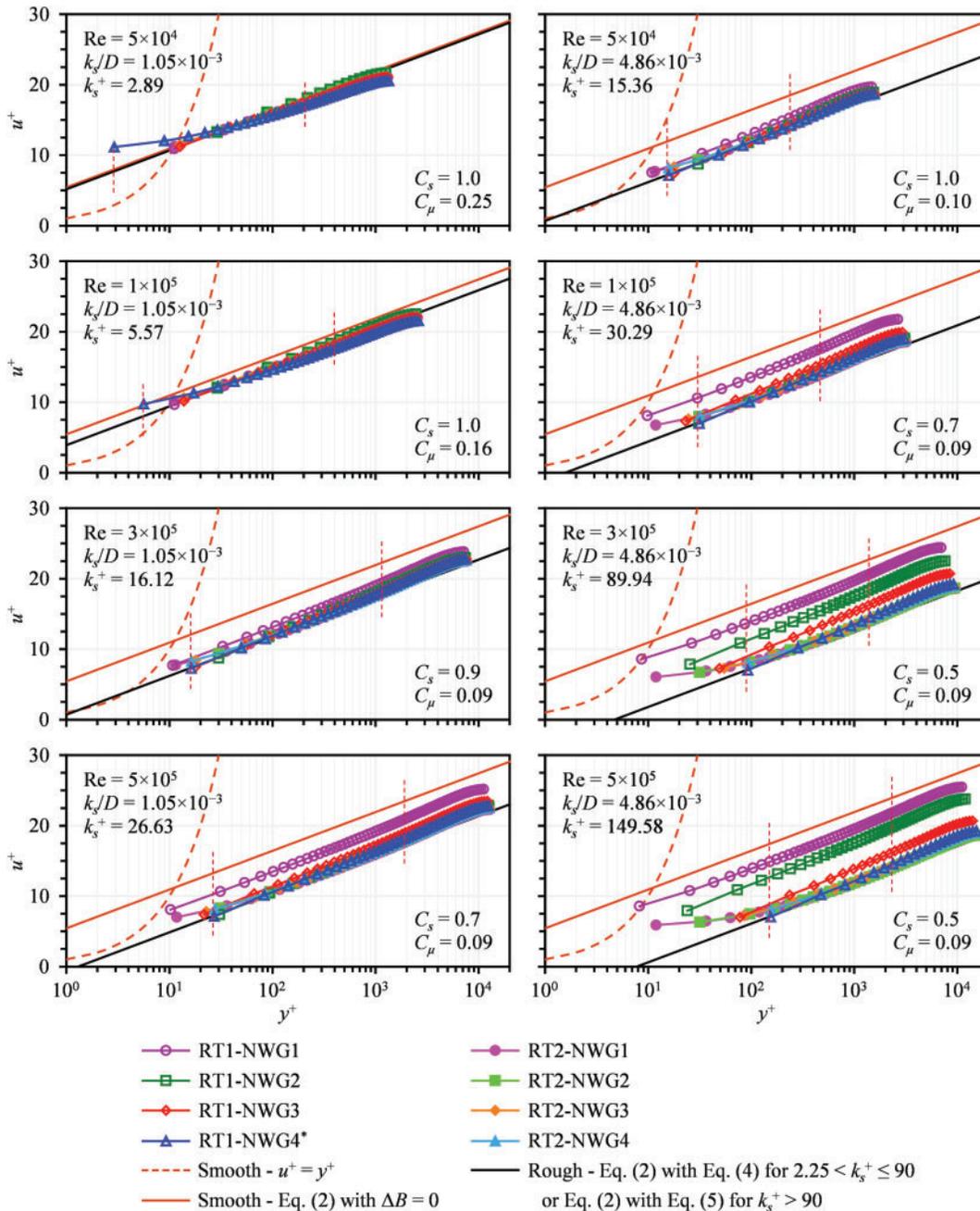
K. Boonsamer, B. Temsiriphan, P. Thongnoi, S. Areerat, E. Bumrungthaichaichan
and S. Wattananusorn,
How can an appropriate CFD model be developed for turbulent flow
in rough pipes?: Evidence from friction factor prediction,
Rev. int. métodos numér. cálc. diseño ing. (2026). Vol.42, (2), 69

Figure 9: Non-dimensional mean velocity profiles of inflectional roughness predicted by different near-wall grid CFD models and roughness treatment approaches with roughness constant of 0.5

K. Boonsamer, B. Temsiriphan, P. Thongnoi, S. Areerat, E. Bumrungthaichaichan
and S. Wattananusorn,
How can an appropriate CFD model be developed for turbulent flow
in rough pipes?: Evidence from friction factor prediction,
Rev. int. métodos numér. cálc. diseño ing. (2026). Vol.42, (2), 69

Figure 10: Non-dimensional mean velocity profiles of monotonic roughness predicted by different near-wall grid CFD models and roughness treatment approaches with appropriate roughness and turbulence model constants

K. Boonsamer, B. Temsiriphan, P. Thongnoi, S. Areerat, E. Bumrungthaichaichan
and S. Wattananusorn,
How can an appropriate CFD model be developed for turbulent flow
in rough pipes?: Evidence from friction factor prediction,
Rev. int. métodos numér. cálc. diseño ing. (2026). Vol.42, (2), 69

From Figs. 9 and 10, the results reveal that the predicted non-dimensional mean velocity profiles of the NWG4s developed by two different roughness treatment approaches agree well with the rough wall logarithmic-law profiles for both roughness types, especially for roughness Reynolds numbers greater than 11.225, and exhibit better agreement than those of the other CFD models, consistent with the Fanning friction factor predictions. Even though Eqs. (2)–(5) were employed by the wall functions to calculate the mean velocities at the first near-wall computing nodes, the RANS equations with the standard k-epsilon model predicted similar non-dimensional mean velocity profiles to those described by these equations due to the accurate near-wall velocity prediction and the use of high-quality grids.

For roughness Reynolds numbers below 11.225, the NWG4s predict identical non-dimensional mean velocity profiles for two different roughness treatment approaches. However, the predicted mean axial velocities in the near-wall region of NWG4s developed by two different roughness treatment approaches deviate from the rough wall logarithmic-law profiles because for near-wall computing nodes located below a dimensionless wall distance of 11.225, the scalable wall functions use dimensionless wall distance of 11.225 for the near-wall mean velocity computation instead of the actual dimensionless wall distance of the near-wall grid [27]. In other words, for the same grid generation, the predicted non-dimensional mean velocity profiles of the two roughness treatment approaches remain identical and deviate from the rough wall logarithmic-law profile in the near-wall region as long as the dimensionless wall distances of the near-wall grids determined by these approaches are smaller than 11.225. To obtain better agreement in the mean axial velocity prediction for roughness Reynolds number below 11.225, the near-wall computing nodes should be located at the dimensionless wall distance of 11.225 or higher, as demonstrated by NWG1, NWG2, and NWG3; however, this leads to a loss of accuracy in the Fanning friction factor prediction.

For roughness Reynolds numbers above 11.225, the mean axial velocities predicted by NWG4s developed by RT1 slightly differ from those obtained by RT2 but show better agreement with the rough wall logarithmic-law profiles across the logarithmic region, from its lower to upper bounds. The higher mean axial velocities predicted by RT2 near the lower bound of the logarithmic region are attributed to the half roughness element height blocked flow assumption, in which the higher dimensionless wall distance is used for near-wall mean velocity computation of the wall functions as previously described in Section 2.

According to the present predicted non-dimensional mean velocity profiles, it can be summarized that for roughness Reynolds numbers above 11.225, the NWG4s with RT1 are preferred for both inflectional and monotonic roughness types, as they exhibit slightly better agreement in mean velocity prediction near the lower bound of the logarithmic region than NWG4s developed by RT2. However, for roughness Reynolds numbers below 11.225, the selection of an appropriate CFD model depends on the intended focus, either on Fanning friction factor analysis (NWG4) or on mean velocity prediction (NWG1, NWG2, and NWG3).

5 Conclusions

The present CFD study investigates an appropriate RANS equation-based CFD model employing the standard k-epsilon model with scalable wall functions for turbulent flows in inflectional and monotonic rough pipes, mainly by analyzing the predicted Fanning friction factors obtained by four different near-wall grid CFD models and two roughness treatment approaches. Four Reynolds numbers and two relative roughness values, corresponding to eight roughness Reynolds numbers for each roughness type, were simulated. Grid independent solutions and quantitative grid convergence were successfully achieved by comparing normalized mean velocity profiles and analyzing GCI of

K. Boonsamer, B. Temsiriphan, P. Thongnoi, S. Areerat, E. Bumrungthaichaichan
and S. Wattananusorn,
How can an appropriate CFD model be developed for turbulent flow
in rough pipes?: Evidence from friction factor prediction,
Rev. int. métodos numér. cálc. diseño ing. (2026). Vol.42, (2), 69

Fanning friction factors for turbulent pipe flows with Reynolds numbers of 5×10^4 and 5×10^5 simulated by three different grid resolutions. For model validation, the predicted normalized mean velocity profiles for Reynolds numbers of 5×10^4 and 5×10^5 agreed well with the previous measured data of Laufer [29].

The Fanning friction factors predicted by 208 CFD simulations (32 from previous works [25,26] and 176 from the present study) were compared to those of inflectional correlation of Afzal [8] and the monotonic correlation of Colebrook-White [4] to identify appropriate CFD models for turbulent flow in rough pipes. In addition, 124 of 208 CFD simulations (32 from previous works [26] and 92 from the present study) were analyzed by comparing the predicted non-dimensional mean velocity profiles with the rough wall logarithmic-law profiles to assess the capability of the CFD models in predicting mean velocity within the logarithmic region. Finally, the conclusions have been drawn to obtain appropriate CFD models developed by the standard k-epsilon model with scalable wall functions for turbulent flows in inflectional and monotonic rough pipes as follows:

According to Fanning friction factor comparisons and NMSE analysis, the near-wall grid sizes obtained by dimensionless wall distance of roughness Reynolds number (NWG4), in which the proper near-wall grid size is twice the roughness height for cell-center-based CFD codes, are only recommended for predicting Fanning friction factors of inflectional and monotonic roughness types. This recommended near-wall grid size contradicts the suggestion of Johansson [16], who suggested that the near-wall grid size may be larger than twice the roughness height. It is noted that larger near-wall grid sizes can accurately predict non-dimensional mean velocity profiles in the logarithmic region for roughness Reynolds numbers below 11.225; however, this should be applied with caution, as it may reduce the accuracy of the Fanning friction factor prediction.

Both RT1 and RT2 accurately predict the Fanning friction factors. However, RT1 offers superior accuracy in mean velocity prediction across the logarithmic region. Therefore, RT1 is recommended for accurately predicting both Fanning friction factor and mean velocity profile.

The default values of 0.5 and 0.09 for the roughness and turbulence model constants are adequate for simulating inflectional roughness. In contrast, monotonic roughness requires higher roughness and turbulence model constants to capture the effects of non-uniform roughness, particularly from the middle to the lower end of the transitionally rough regime. Based on Fanning friction factor comparisons, the present study identifies the roughness and turbulence model constants required for modelling turbulent flows in both inflectional and monotonic rough pipes as summarized in Table 5. It is noted that the roughness Reynolds numbers of 16 and 70 in Table 5, adopted as reference values for setting the roughness and turbulence model constants in the transitionally rough regime, were determined from the present CFD results and from the fully rough regime criterion reported in the previous works [1,47,48], respectively.

The present work successfully provides an appropriate CFD model for turbulent rough pipe flow, which can be effectively extended to other rough surface types, especially for guiding the specification of roughness and turbulence model constants in the transitionally rough regime. Furthermore, the findings of this work are also valuable for simulating other flow situations involving rough surfaces, where similar modelling concepts can be applied. For future work, further studies on heat transfer, non-Newtonian fluids (e.g., pseudoplastic and dilatant fluids), and turbulence models (e.g., k-omega and SST k-omega models) are required to establish more comprehensive guidelines for CFD modeling of turbulent rough pipe flows.

K. Boonsamer, B. Temsiriphan, P. Thongnoi, S. Areerat, E. Bumrungthaichaichan and S. Wattananusorn,
How can an appropriate CFD model be developed for turbulent flow in rough pipes?: Evidence from friction factor prediction,
Rev. int. métodos numér. cálc. diseño ing. (2026). Vol.42, (2), 69

Table 5: Recommended roughness and turbulence model constants for inflectional and monotonic roughness types

Parameter	Roughness Reynolds number	Inflectional roughness	Monotonic roughness
Roughness constant	$2.25 < k_s^+ < 70$	0.5	0.5–1.0
	$k_s^+ \geq 70$	0.5	0.5
Turbulence model constant	$2.25 < k_s^+ < 16$	0.09	>0.09
	$k_s^+ \geq 16$	0.09	0.09

Author Contributions: The authors confirm contribution to the paper as follows: Conceptualization, Kraiwit Boonsamer and Eakarach Bumrungthaichaichan; methodology, Kraiwit Boonsamer and Eakarach Bumrungthaichaichan; software, Kraiwit Boonsamer; validation, Eakarach Bumrungthaichaichan and Santi Wattananusorn; formal analysis, Kraiwit Boonsamer, Barami Temsiriphan, Piyawut Thongnoi, Surat Areerat and Eakarach Bumrungthaichaichan; investigation, Kraiwit Boonsamer; resources, Kraiwit Boonsamer; data curation, Kraiwit Boonsamer; writing—original draft preparation, Kraiwit Boonsamer and Eakarach Bumrungthaichaichan; writing—review and editing, Barami Temsiriphan, Piyawut Thongnoi, Surat Areerat, Eakarach Bumrungthaichaichan and Santi Wattananusorn; visualization, Kraiwit Boonsamer and Eakarach Bumrungthaichaichan; supervision, Eakarach Bumrungthaichaichan and Santi Wattananusorn; project administration, Eakarach Bumrungthaichaichan. All authors reviewed the results and approved the final version of the manuscript.

Availability of Data and Materials: The data that support the findings of this study are available from the Corresponding Author, Eakarach, upon reasonable request.

Ethics Approval: Not applicable.

Conflicts of Interest: The authors declare no conflicts of interest to report regarding the present study.

References

1. Nikuradse J. Strömungsgesetze in rauhen Rohren. Forsch Auf Dem Geb Des Ingenieurwesens. 1933;4(B):VDI-Forschungsheft 361. (In German).
2. Hager WH, Liiv U. Johann nikuradse-hydraulic experimenter. J Hydraul Res. 2008;46(4):435–44. doi:10.1080/00221686.2008.9521880.
3. Gioia G, Chakraborty P. Turbulent friction in rough pipes and the energy spectrum of the phenomenological theory. Phys Rev Lett. 2006;96(4):044502. doi:10.1103/physrevlett.96.044502.
4. Colebrook CF. Turbulent flow in pipes, with particular reference to the transition region between the smooth and rough pipe laws. J Inst Civ Eng. 1939;11(4):133–56. doi:10.1680/ijoti.1939.13150.
5. Moody LF. Friction factors for pipe flow. ASME Trans. 1944;66:671–84.

K. Boonsamer, B. Temsiriphan, P. Thongnoi, S. Areerat, E. Bumrungthaichaichan
and S. Wattananusorn,
How can an appropriate CFD model be developed for turbulent flow
in rough pipes?: Evidence from friction factor prediction,
Rev. int. métodos numér. cálc. diseño ing. (2026). Vol.42, (2), 69

6. McGovern J. Technical note: friction diagrams for pipe flow. Dublin, Ireland: Dublin Institute of Technology; 2011.

7. Allen JJ, Shockling MA, Kunkel GJ, Smits AJ. Turbulent flow in smooth and rough pipes. Phil Trans R Soc A. 2007;365(1852):699–714. doi:10.1098/rsta.2006.1939.

8. Afzal N. Friction factor directly from transitional roughness in a turbulent pipe flow. J Fluids Eng. 2007;129(10):1255–67. doi:10.1115/1.2776961.

9. Bumrungthaichaichan E. How can the appropriate near-wall grid size for gas cyclone CFD simulation be estimated? Powder Technol. 2022;396:327–44. doi:10.1016/j.powtec.2021.10.031.

10. Foroozesh J, Parvaz F, Hosseini SH, Ahmadi G, Elsayed K, Babaoğlu NU. Computational fluid dynamics study of the impact of surface roughness on cyclone performance and erosion. Powder Technol. 2021;389:339–54. doi:10.1016/j.powtec.2021.05.041.

11. Dehdarinejad E, Bayareh M. Impact of non-uniform surface roughness on the erosion rate and performance of a cyclone separator. Chem Eng Sci. 2022;249:117351. doi:10.1016/j.ces.2021.117351.

12. Geete A, Pathak R. Effect of surface roughness on the performance of heat exchanger. SN Appl Sci. 2019;1:901. doi:10.1007/s42452-019-0954-x.

13. Ali AA, Alfarge D, Lafta AM, Hasan MI, Rashid FL. Numerical investigation for the effects of surface roughness in counter flow microchannel heat exchanger with different channels geometries. Discov Appl Sci. 2024;6:459. doi:10.1007/s42452-024-06132-5.

14. Ibrahim MB, Veluri S, Simon T, Gedeon D. CFD modeling of surface roughness in laminar flow. In: Proceedings of the 2nd International Energy Conversion Engineering Conference; 2004 Aug 16–19; Providence, RI, USA. doi:10.2514/6.2004-5585.

15. Vijiapurapu S, Cui J. Performance of turbulence models for flows through rough pipes. Appl Math Model. 2010;34(6):1458–66. doi:10.1016/j.apm.2009.08.029.

16. Johansson C. Optimization of wall parameters using CFD [master's thesis]. Stockholm, Sweden: Royal Institute of Technology; 2014. 14 p.

17. Haroon A, Ahmad S, Hussain A. CFD prediction of loss coefficient in straight pipes. In: Garg V, Singh VP, Raj V, editors. Development of water resources in India. Proceedings of the National Conference on Water Resources and Hydropower (WRHP-2016); 2016 Jun 17–18; Dehradun, India. Cham, Switzerland: Springer International Publishing; 2017. p. 477–85. doi:10.1007/978-3-319-55125-8_41.

18. Abdelrazek AH, Alawi OA, Kazi SN, Yusoff N, Chowdhury Z, Sarhan AAD. A new approach to evaluate the impact of thermophysical properties of nanofluids on heat transfer and pressure drop. Int Commun Heat Mass Transf. 2018;95:161–70. doi:10.1016/j.icheatmasstransfer.2018.05.002.

19. Aldlemy MS, Ahammed SJ, Obando ED, Bayatvarkeshi M. Numerical simulation on the effect of pipe roughness in turbulent flow. Knowl -Based Eng Sci. 2022;3(1):37–44. doi:10.51526/kbes.2022.3.1.37-44.

20. Loyseau XF, Verdin PG, Brown LD. Scale-up and turbulence modelling in pipes. J Petrol Sci Eng. 2018;162:1–11. doi:10.1016/j.petrol.2017.12.019.

21. Blasius H. Das aehnlichkeitsgesetz Bei reibungsvorgängen in Flüssigkeiten. In: Ingenieure VD, editor. Mitteilungen über forschungsarbeiten auf dem gebiete des ingenieurwesens. Vol. 131. Berlin/Heidelberg, Germany: Springer; 1913. p. 1–41. (In German). doi:10.1007/978-3-662-02239-9_1.

22. Bumrungthaichaichan E, Unaprom P, Sathianchok P, Wattananusorn S. On the semi-analytical solution of displacement thickness in a laminar streamwise corner flow assisted by computational fluid dynamics simulation. J Comput Theor Transp. 2023;52(1):42–54. doi:10.1080/23324309.2023.2171063.

23. Temsiriphan B. Near-wall grid size estimation for computational fluid dynamics simulation of turbulent flow in straight rough pipe [master's thesis]. Bangkok, Thailand: King Mongkut's Institute of Technology Ladkrabang; 2021. 55 p. (In Thai).

24. ANSYS Inc. ANSYS fluent user's guide: release 15.0. Canonsburg, PA, USA: ANSYS Inc; 2014.

K. Boonsamer, B. Temsiriphan, P. Thongnoi, S. Areerat, E. Bumrungthaichaichan
and S. Wattananusorn,
How can an appropriate CFD model be developed for turbulent flow
in rough pipes?: Evidence from friction factor prediction,
Rev. int. métodos numér. cálc. diseño ing. (2026). Vol.42, (2), 69

25. Boonsamer K, Thongnoi P, Bumrungthaichaichan E, Wattananusorn S. Effect of near-wall grid size for computational fluid dynamics simulation of turbulent flow in a rough surface pipe. In: Proceedings of the Operations Research Network 2025 Conference; 2025 Mar 26–28; Bangkok, Thailand. (In Thai).

26. Boonsamer K. Near-wall grid size estimation for computational fluid dynamics simulation of turbulent flow in an inflectional rough surface pipe [master's thesis]. Bangkok, Thailand: King Mongkut's Institute of Technology Ladkrabang; 2025. 51 p. (In Thai).

27. ANSYS Inc. ANSYS fluent theory guide: release 15.0. Canonsburg, PA, USA: ANSYS Inc; 2013.

28. Cebeci T, Bradshaw P. Momentum transfer in boundary layers. New York, NY, USA: Hemisphere Publishing Corporation; 1977.

29. Laufer J. The structure of turbulence in fully developed pipe flow (NACA-TR-1174). Washington, DC, USA: National Advisory Committee for Aeronautics; 1954.

30. Tongpun P, Bumrungthaichaichan E, Wattananusorn S. Investigation of entrance length in circular and noncircular conduits by computational fluid dynamics simulation. Songklanakarin J Sci Technol. 2014;36(4):471–5.

31. Khoshvaght-Aliabadi M, Salami M. Turbulent flow of Al_2O_3-water nanofluid through plate-fin heat exchanger (PFHE) with offset-strip channels. Therm Sci Eng Prog. 2018;6:164–76. doi:10.1016/j.tsep.2018.04.001.

32. Hirpa MM, Arnipally SK, Kuru E. Effect of the particle size on the near-wall turbulence characteristics of the polymer fluid flow and the critical velocity required for particle removal from the sand bed deposited in horizontal wells. Energies. 2020;13(12):3172. doi:10.3390/en13123172.

33. Sardar MAI, Rahman M, Rubini P. Enhancing thermal-hydraulic performance in nuclear reactor subchannels with Al_2O_3 nanofluids: a CFD analysis. Energies. 2024;17(21):5486. doi:10.3390/en17215486.

34. Li H, Li Y, Huang B, Xu T. Flow characteristics of the entrance region with roughness effect within rectangular microchannels. Micromachines. 2020;11(1):30. doi:10.3390/mi11010030.

35. Praks P, Brkić D. Review of new flow friction equations: constructing Colebrook's explicit correlations accurately. Rev Int Metod Numer Calc Dise. 2020;36(3):41. doi:10.23967/j.rimni.2020.09.001.

36. Bumrungthaichaichan E. A note of caution on numerical scheme selection: Evidence from cyclone separator CFD simulations with appropriate near-wall grid sizes. Powder Technol. 2023;427:118713. doi:10.1016/j.powtec.2023.118713.

37. ANSYS Inc. Introduction to ANSYS fluent 15.0 release—workshop 04 fluid flow around the NACA0012 airfoil. Canonsburg, PA, USA: ANSYS Inc; 2014.

38. Bumrungthaichaichan E, Ruangtrakoon N, Thongtip T. Performance investigation for CRMC and CPM ejectors applied in refrigeration under equivalent ejector geometry by CFD simulation. Energy Rep. 2022;8:12598–617. doi:10.1016/j.egyr.2022.09.042.

39. Bumrungthaichaichan E, Namkanisorn A, Wattananusorn S. CFD modelling of pump-around jet mixing tanks: a discrepancy in concentration profiles. J Chin Inst Eng. 2018;41(7):612–21. doi:10.1080/02533839.2018.1530956.

40. Wattananusorn S. New space-averaging procedure for inhomogeneous flow fields using balance equation formulations. Proc Inst Mech Eng Part C J Mech Eng Sci. 2006;220(9):1363–74. doi:10.1243/09544062c06605.

41. Stoff H. Energy-based averaging by applying directive VDI 4675 to various flow sample cases. Int J Eng Res-Online. 2016;4(3):522–30.

42. Builtjes PJH. Memory effects in turbulent flows [doctoral thesis]. Delft, The Netherlands: Delft University of Technology; 1977. 134 p.

43. Jiménez J. Turbulent flows over rough walls. Annu Rev Fluid Mech. 2004;36:173–96. doi:10.1146/annurev.fluid.36.050802.122103.

K. Boonsamer, B. Temsiriphan, P. Thongnoi, S. Areerat, E. Bumrungthaichaichan
and S. Wattananusorn,
How can an appropriate CFD model be developed for turbulent flow
in rough pipes?: Evidence from friction factor prediction,
Rev. int. métodos numér. cálc. diseño ing. (2026). Vol.42, (2), 69

44. Flack KA, Schultz MP. Roughness effects on wall-bounded turbulent flows. Phys Fluids. 2014;26:101305. doi:10.1063/1.4896280.

45. Chan L, MacDonald M, Chung D, Hutchins N, Ooi A. A systematic investigation of roughness height and wavelength in turbulent pipe flow in the transitionally rough regime. J Fluid Mech. 2015;771:743–77. doi:10.1017/jfm.2015.172.

46. Wattananusorn S. Non-decay of complex scalar field fluctuations in isotropic turbulence. Chem Eng Sci. 2020;218:115463. doi:10.1016/j.ces.2019.115463.

47. Shockling MA, Allen JJ, Smits AJ. Roughness effects in turbulent pipe flow. J Fluid Mech. 2006;564: 267–85. doi:10.1017/s0022112006001467.

48. Schultz MP, Flack KA. The rough-wall turbulent boundary layer from the hydraulically smooth to the fully rough regime. J Fluid Mech. 2007;580:381–405. doi:10.1017/s0022112007005502.

49. Botros KK. Experimental investigation into the relationship between the roughness height in use with nikuradse or colebrook roughness functions and the internal wall roughness profile for commercial steel pipes. J Fluids Eng. 2016;138(8):081202. doi:10.1115/1.4032601.

50. Bhaganagar K, Chau L. Characterizing turbulent flow over 3-D idealized and irregular rough surfaces at low Reynolds number. Appl Math Model. 2015;39(22):6751–66. doi:10.1016/j.apm.2015.02.024.

51. Ma R, Alamé K, Mahesh K. Direct numerical simulation of turbulent channel flow over random rough surfaces. J Fluid Mech. 2021;908:A40. doi:10.1017/jfm.2020.874.

52. Santiago JL, Martilli A, Martín F. CFD simulation of airflow over a regular array of cubes. Part I: three-dimensional simulation of the flow and validation with wind-tunnel measurements. Bound Layer Meteor. 2007;122:609–34. doi:10.1007/s10546-006-9123-z.

53. Wu L, Hang J, Wang X, Shao M, Gong C. APFoam 1.0: integrated computational fluid dynamics simulation of O_3–NO_x–volatile organic compound chemistry and pollutant dispersion in a typical street canyon. Geosci Model Dev. 2021;14(7):4655–81. doi:10.5194/gmd-14-4655-2021.

54. Thongnoi P, Chandra-ambhorn W, Chalermsinsuwan B, Wattananusorn S, Wongpromrat P, Bumrungthaichaichan E. RANS equation-based gas cyclone separator CFD simulation: an appropriate time step size. Chem Eng Trans. 2024;113:649–54. doi:10.3303/CET24113109.

55. Hultmark M, Vallikivi M, Bailey SCC, Smits AJ. Logarithmic scaling of turbulence in smooth- and rough-wall pipe flow. J Fluid Mech. 2013;728:376–95. doi:10.1017/jfm.2013.255.

56. Marusic I, Monty JP, Hultmark M, Smits AJ. On the logarithmic region in wall turbulence. J Fluid Mech. 2013;716:R3. doi:10.1017/jfm.2012.511.

57. Brereton GJ, Jouybari MA, Yuan J. Toward modeling of turbulent flow over surfaces of arbitrary roughness. Phys Fluids. 2021;33:065121. doi:10.1063/5.0051097.

58. Womack KM, Volino RJ, Meneveau C, Schultz MP. Turbulent boundary layer flow over regularly and irregularly arranged truncated cone surfaces. J Fluid Mech. 2022;933:A38. doi:10.1017/jfm.2021.946.